14th European Signal Processing Conference (EUSIPCO 2006), Florence, Italy, September 4-8, 2006, copyright by EURASIP

TIME-VARYING CHANNEL MODEL EFFICIENCY

Scott Rickard[†]*, Konstantinos Drakakis*[‡]*, Nikolaos Tsakalozos*[†]

School of Electronic, Electrical & Mechanical Engineering
University College Dublin
IRELAND

[‡]School of Mathematics
University of Edinburgh
SCOTLAND

ABSTRACT

We consider the form of a physically motivated simple one path time-varying channel in the time-varying impulse response, time-frequency characterization and time-scale characterization settings. Our goal is to determine which setting allows for the most efficient (i.e., sparse) discrete channel representation as a function of input signal bandwidth. We measure how well the input-output relationship is captured by the discrete coefficients for modulated Gaussian pulse input signals and examine how the performance of the discrete channel models varies with the bandwidth of the input signal.

1. OVERVIEW

Which discrete time-varying channel model is the most efficient? Several channel models exist, but which of them captures most efficiently the action of the channel? We consider in this work three models: a time domain characterization (i.e., the time-varying impulse response), a time-frequency characterization, and a time-scale characterization. The time-domain characterization represents the channel output as a series of weighted discrete delayed versions of the input signal, the time-frequency characterization represents the channel output as a series of weighted discrete delayed and frequency shifted versions of the input signal, and the time-scale characterization represents the channel output as a series of weighted discrete delayed and dilated versions of the input signal. Given that practical receivers must model the channel using a limited number of channel coefficients, we examine how accurately the channel is captured for the three models as a function of the number of coefficients available.

In continuous time, the three models considered here are time-domain,

$$y(t) = \int h(t,\tau)x(t-\tau)\mathrm{d}\tau, \tag{1}$$

time-frequency domain,

$$y(t) = \iint S(\theta,\tau)x(t-\tau)e^{j2\pi\theta t}\mathrm{d}\tau\mathrm{d}\theta, \tag{2}$$

and time-scale domain,

$$y(t) = \iint \mathcal{L}(a,b,t)\frac{1}{\sqrt{|a|}}x\left(\frac{t-b}{a}\right)\mathrm{d}a\mathrm{d}b. \tag{3}$$

The three models each have discrete expansions. They are time-domain,

$$y(t) = \sum_n \hat{h}_n(t)x\left(t-\frac{n}{W}\right) \tag{4}$$

where

$$\hat{h}_n(t) = \int h(t,\tau)\frac{\sin\left(\pi W\left(\tau-\frac{n}{W}\right)\right)}{\pi W\left(\tau-\frac{n}{W}\right)}\mathrm{d}\tau; \tag{5}$$

time-frequency domain,

$$y(t) = \sum_m\sum_n \hat{S}_{m,n}x\left(t-\frac{n}{W}\right)e^{j2\pi mt/T} \tag{6}$$

where

$$\hat{S}_{m,n} = \iint S(\theta,\tau)\mathrm{sinc}\left(n-\tau W\right)\mathrm{sinc}\left(m-\theta T\right)e^{-j\pi(m-\theta T)}\mathrm{d}\theta\mathrm{d}\tau; \tag{7}$$

and time-scale domain,

$$y(t) = \sum_{m,n}\frac{\hat{\mathcal{L}}_{m,n}(t)}{a_0^{m/2}}x\left(\frac{t-nb_0a_0^m}{a_0^m}\right) \tag{8}$$

where

$$\hat{\mathcal{L}}_{m,n}(t) = \iint \mathcal{L}(a,b,t)\mathrm{sinc}\left(m-\frac{\ln a}{\ln a_0}\right)\mathrm{sinc}\left(n-\frac{b}{ab_0}\right)\mathrm{d}a\mathrm{d}b. \tag{9}$$

In the above models, W, T, a_0, b_0 are related to channel and signal characteristics [1–4]. Each of these three models and their discrete expansions have been studied, in some cases, for nearly 50 years [1–10]. In each case, the channel is captured by a set of coefficients ($\hat{h}_n(t)$, $\hat{S}_{m,n}$, and $\hat{\mathcal{L}}_{m,n}(t)$).

In a previous paper [10], we evaluated the efficiency of the channel representation by looking at how well the channel was reconstructed when only a limited number of channel coefficients were available. In this paper, we take a different approach to measuring the efficiency, concentrating on how well the channel coefficients reconstruct a Gaussian pulse. The channel we consider is one where a transmitter and receiver move with constant radial velocity relative to one another. For ease of presentation, we consider in this work exclusively that the signal is an audio signal so that we may ignore relativistic effects. This simplifies the derivation of the Doppler effect, although the resulting channel for electromagnetic waves has a similar, but not identical, form. The results presented here can be extended to apply to wireless signals in a straightforward manner.

The paper is organized as follows. In Section 2 we derive the physically motivated one path Doppler effect non-relativistic channel. In Section 3 we derive the continuous time characterizations of this channel. In Section 4 we derive the channel coefficients for the simple channel. In Section 5 we analyze the efficiency of the channel representations as a function of the number of channel coefficients for the three discrete models when reconstructing a Gaussian pulse and analyze the results specifically as a function of the bandwidth of the pulse.

2. THE CLASSIC DOPPLER EFFECT

The treatment in this section is the classic treatment of the Doppler effect, as opposed to relativistic. Consider a source,

$x(t)$ located at the origin moving to the right with velocity v_x. The position of the source is described by,

$$p_x(t) = v_x t \tag{10}$$

Consider a receiver, $y(t)$ located initially at a distance d_0 from the origin along the positive x-axis moving to the right with velocity v_y. The position of the receiver is described by,

$$p_y(t) = v_y t + d_0 \tag{11}$$

We define τ to be the time delay such that the source signal traveling with speed c_0 emitted at time $t-\tau$ reaches the receiver at time t. Clearly, the distance that the signal travels must equal the difference between the current receiver position and position of the source τ seconds ago. This can be described,

$$\begin{aligned} c_0\tau &= |p_y(t) - p_x(t-\tau)| &(12)\\ &= |v_y t + d_0 - v_x(t-\tau)|. &(13)\end{aligned}$$

Solving for τ,

$$\text{Case 1:}\quad p_y(t) > p_x(t-\tau),\quad \tau = \frac{(v_y - v_x)t + d_0}{c_0 - v_x}, \tag{14}$$

$$\text{Case 2:}\quad p_y(t) < p_x(t-\tau),\quad \tau = \frac{(-v_y + v_x)t - d_0}{c_0 + v_x} \tag{15}$$

Substituting these back into (13) we obtain (assuming $|v_x| < c_0$),

$$\text{Case 1:}\quad p_y(t) > p_x(t),\quad \tau = \frac{(v_y - v_x)t + d_0}{c_0 - v_x}, \tag{16}$$

$$\text{Case 2:}\quad p_y(t) < p_x(t),\quad \tau = \frac{(-v_y + v_x)t - d_0}{c_0 + v_x}. \tag{17}$$

Assuming that the amplitude decays with the reciprocal of distance, the input output mapping is,

$$\begin{aligned} y(t) &= \frac{1}{|p_y(t) - p_x(t-\tau)|} x(t-\tau) &(18)\\ &= \begin{cases} \frac{1-v_x/c_0}{d_0-(v_x-v_y)t} x\left(\frac{t-\frac{d_0}{c_0-v_y}}{A}\right) & : \quad p_y(t) > p_x(t) \\ \frac{1+v_x/c_0}{(v_x-v_y)t-d_0} x\left(\frac{t+\frac{d_0}{c_0+v_y}}{B}\right) & : \quad p_y(t) < p_x(t) \end{cases} &(19)\end{aligned}$$

where $A = \frac{c_0-v_x}{c_0-v_y}$ and $B = \frac{c_0+v_x}{c_0+v_y}$. The change in Doppler effect from contraction to expansion occurs when the transmitter and receiver are collocated ($p_y(t) = p_x(t)$).

In the above derivation we ignored relativistic considerations, which is reasonable assuming that, $|v_x| \ll c$, $|v_y| \ll c$, and $c_0 \ll c$, where c is the speed of light. Note the lack of symmetry with v_x and $-v_y$. That is, the effect of x moving toward stationary y with speed v is different than the effect of y moving toward stationary x with speed v. This is not the case when $c_0 = c$. That is, when the speed of signal propagation is the speed of light, it is impossible to for either x or y to determine whether x is moving toward stationary y or y is moving toward stationary x due to relativistic effects [11]. Also note that $v_x = v$ and $v_x = -v$ do not shift the frequency by the same amount. This difference remains true even when $c_0 = c$.

3. CONTINUOUS CHANNEL MODELS OF THE CLASSIC DOPPLER EFFECT

We now derive the continuous time models (in time, time-frequency, and time-scale) for the physically motivated one-path constant radial velocity channel described by (19). It is clear that the classic Doppler effect described by Equation 19 has a form similar to the time-scale characterization described by Equation 3 in that the output signal is a time-delayed and time-scaled version of the input signal, so we first map (19) to time-scale and obtain

$$\mathcal{L}(a,b,t) = \sqrt{|A|}\frac{1 - v_x/c_o}{d_0 - (v_x - v_y)t}\delta\left(a - A\right)\delta\left(b - \frac{d_0}{c_0 - v_y}\right) \tag{20}$$

when $p_y(t) > p_x(t)$ and

$$\mathcal{L}(a,b,t) = \sqrt{|B|}\frac{1 + v_x/c_0}{(v_x - v_y)t - d_0}\delta\left(a - B\right)\delta\left(b + \frac{d_0}{c_0 + v_y}\right) \tag{21}$$

when $p_y(t) < p_x(t)$. Note that the $\mathcal{L}(a,b,t)$ characterization has point support $(a,b) = (A, \frac{d_0}{c_0-v_y})$ for $p_y(t) > p_x(t)$ switching to $(a,b) = (B, -\frac{d_0}{c_0+v_y})$ for $p_y(t) < p_x(t)$ with magnitude changing as a function of time. For $c_0 >> v_x, v_y$, $(A, \frac{d_0}{c_0-v_y}) \approx (1/B, -(-\frac{d_0}{c_0+v_y}))$ so that the switch is from one point (a,b) to approximately $(1/a, -b)$.

For simplicity, we consider exclusively (20) for the rest of this paper as the time-scale model, that is, we assume that $p_y(t) > p_x(t)$ for the period of time we are interested in. Similar results can be achieved in the case of $p_y(t) < p_x(t)$. We can map (20) to time-frequency $\mathcal{S}(\theta,\tau)$ using

$$\mathcal{S}(\theta,\tau) = \iint \sqrt{|a|}\mathcal{L}(a,(1-a)t + a\tau, t)e^{-j2\pi\theta t}\mathrm{d}t\mathrm{d}a \tag{22}$$

from [12] augmented with the dependence on t yielding

$$\mathcal{S}(\theta,\tau) = |C|\frac{1}{c_0\tau}e^{j2\pi C\theta\left(\tau - \frac{d_0}{c_0-v_x}\right)} \tag{23}$$

where $C = \frac{c_0-v_x}{v_x-v_y}$.

We can further map this to the time-domain characterization $h(t,\tau)$ via the defining relationship between $h(t,\tau)$ and $\mathcal{S}(\theta,\tau)$,

$$h(t,\tau) = \int \mathcal{S}(\theta,\tau)e^{j2\pi\theta t}\mathrm{d}\theta, \tag{24}$$

and we obtain,

$$h(t,\tau) = |C|\,\frac{1}{c_o\tau}\delta\left(t + \frac{(c_0 - v_x)\tau - d_0}{v_x - v_y}\right). \tag{25}$$

We summarize all three equivalent input-output relationship for this simple physical channel in Table 1.

4. DISCRETE CHANNEL MODELS OF THE CLASSIC DOPPLER EFFECT

In [4, 12] the mapping among the continuous models; (1), (2), and (3); is established. These mappings are developed independent of the signaling assumptions. Each continuous model has a corresponding discrete representation; (4,5), (6,7), and (8,9) respectively; which arises from specific assumptions about the transmit signals and how they are analyzed at the receiver. In [4] in particular, the following interpretation is established:

- time-domain (4) and (5) assume frequency bandlimited transmit signals with bandwidth W and has no constraint on the receiver,
- time-frequency domain (6) and (7) assume frequency bandlimited transmit signals with bandwidth W analyzed at the receiver for a finite time interval T, and

time	$y(t) = \int \left\|\frac{c_0 - v_x}{v_x - v_y}\right\| \frac{1}{c_o \tau} \delta\left(t + \frac{(c_0 - v_x)\tau - d_0}{v_x - v_y}\right) x(t-\tau) \mathrm{d}\tau$
time-frequency	$y(t) = \iint \left\|\frac{c_0 - v_x}{v_x - v_y}\right\| \frac{1}{c_0 \tau} e^{j2\pi\theta \frac{(c_0 - v_x)\tau - d_0}{v_x - v_y}} e^{j2\pi t\theta} x(t-\tau) \mathrm{d}\tau \mathrm{d}\theta$
time-scale	$y(t) = \iint \sqrt{\left\|\frac{c_0 - v_x}{c_0 - v_y}\right\|} \frac{1 - v_x/c_o}{d_0 - (v_x - v_y)t} \delta\left(a - \frac{c_0 - v_x}{c_0 - v_y}\right) \delta\left(b - \frac{d_0}{c_0 - v_y}\right) \frac{1}{\sqrt{\|a\|}} x\left(\frac{t-b}{a}\right) \mathrm{d}a\mathrm{d}b$

Table 1: Summary of continuous time models of the classic Doppler effect.

- time-scale domain (8) and (9) assume frequency bandlimited transmit signals with bandwidth $1/b_0$ received at the receiver for a finite scale (Mellin) domain interval $1/\ln a_0$.

We now map the continuous models to their discrete counterparts by substituting (20), (23), and (25) into their respective coefficient equations (9), (7), and (5). The time-domain and time-scale domain coefficients simplify in a straightforward manner. In the time-frequency case,

$$\hat{\mathcal{S}}_{m,n} = \iint \frac{|C|}{c_0 \tau} e^{j2\pi\theta \frac{(c_0 - v_x)\tau - d_0}{v_x - v_y}} e^{-j\pi(m - \theta T)} \cdot \mathrm{sinc}[n - \tau W] \mathrm{sinc}[m - \theta T] \mathrm{d}\tau \mathrm{d}\theta \quad (26)$$

$$= \int_{\frac{d_0 - T(v_x - v_y)}{c_0 - v_x}}^{\frac{d_0}{c_0 - v_x}} \frac{|C|}{c_0 \tau T} e^{j2\pi m \frac{(c_0 - v_x)\tau - d_0}{T(v_x - v_y)}} \mathrm{sinc}[n - \tau W] \mathrm{d}\tau \quad (27)$$

where we have used

$$1_{(-T/2, +T/2)}(\tau) = \int e^{-j2\pi\tau\theta} T \mathrm{sinc}(T\theta) \mathrm{d}\theta \quad (28)$$

The resulting coefficients for all three models are summarized in Table 2.

5. GAUSSIAN PULSES

All three sets of coefficients in Table 2 describe the simple one path channel under consideration. In this section we examine which representation is the most efficient. If we have an unlimited number of coefficients, then all three representations perfectly characterize the channel. However if only a finite number of coefficients are available, it is not possible, in most cases, to perfectly represent the channel and there is some error in the representation. In [10] we quantified this loss by calculating the efficiency of each representation as a function of the number of coefficients available

In this section we will assume that the transmitted signal is of the form:

$$x(t) = \sqrt[4]{\frac{2s}{\pi}} e^{i\omega_0 t} e^{-s(t - t_0)^2}$$

which is known as a Gaussian pulse or a Gabor signal. Notice that the normalization constant is suitably chosen for the signal to have unit energy, and that $|x(t)|$ is symmetric around t_0; similarly, its spectrum $|X(f)|$ is symmetric around ω_0; finally, $s > 0$ is a localization parameter governing the tradeoff between the width of the signal in time and in frequency, according to the Uncertainty Principle.

The output $y(t)$ of the channel, in the time-domain representation, will be given by:

$$y(t) = \sum_n \hat{h}_n(t) x\left(t - \frac{n}{W}\right) = \sqrt[4]{\frac{2s}{\pi}} \frac{1 - \frac{v_x}{c_0}}{d_0 - (v_x - v_y)t} e^{i\omega_0 t} \sum_n \mathrm{sinc}\left[w \frac{d_0 - (v_x - v_y)t}{c_0 - v_x} - n\right] e^{-i\frac{\omega_0}{w} n} e^{-s\left(t - t_0 - \frac{n}{W}\right)^2} \quad (29)$$

In the time-scale domain, we similarly obtain:

$$y(t) = \sum_{m,n} \frac{\hat{\mathcal{L}}_{m,n}(t)}{a_0^{m/2}} x\left(\frac{t - n b_0 a_0^m}{a_0^m}\right) = \sqrt[4]{\frac{2s}{\pi}} \sum_{m,n} \frac{\sqrt{|A|}}{a_0^{\frac{m}{2}}} \frac{1 - \frac{v_x}{c_0}}{d_0 - (v_x - v_y)t} \mathrm{sinc}\left[\frac{\ln|A|}{\ln a_0} - m\right] \mathrm{sinc}\left[\frac{d_0}{b_0(c_0 - v_x)} - n\right] e^{i\omega_0 \frac{t - n b_0 a_0^m}{a_0^m}} e^{-s\left(\frac{t - n b_0 a_0^m}{a_0^m} - t_0\right)^2} \quad (30)$$

Finally, in the time-frequency domain, where we don't have the channel coefficients in closed form, giving a formula for $y(t)$ would not be very helpful; we will obtain the result numerically, using (6).

Recall that the discrete channel expansion relies upon some assumptions on that the appropriate content of the signal in the relevant domain each time (time, frequency, or scale) be finite; as the Gaussian pulse $x(t)$ is infinite in time, frequency, and scale, some aliasing will inevitably occur and the $y(t)$ constructed by the formulas above will in general not coincide exactly with the $y(t)$ produced by (19), which the true channel output. In what follows, we will study the approximation of the channel output by the above formulas, especially in the case when we use finite sums.

In all of the following experiments we used the parameters $v_x = 10$ m/s, $v_y = -5$ m/s, $c_0 = 1500$ m/s, and $d_0 = 100$; and the pulse parameters $\omega_0 = 200Hz$, $s = 2000$, and $t_0 = 0$; we are also careful to select the reconstruction coefficients symmetrically around the largest one. We plot the absolute values of the signals in all cases, as, in general, they are complex-valued.

Figure 1 shows the time domain reconstruction: using only the largest coefficient, corresponding to $n = W\frac{d_0 - (v_x - v_y)t}{c_0 - v_x}$ according to Table 2, the result is not really accurate, although the effort of the sinc coefficient to capture the pulse is evident and quite impressive; but with 3 coefficients the reconstruction is much better, and with more than that practically exact. We also see that the larger the bandwidth W is, the better the match.

Figure 2 shows the time-scale reconstruction; as discretization parameters, according to (8) and (19) we use $a_0 = A$ to capture the dilation exactly and $b_0 = \frac{d_0}{a_0(c_0 - v_y)}$, to capture the time delay: using only the largest coefficient, corresponding, again according to Table 2, to $n = \left[\frac{d_0}{b_0(c_0 - v_x)}\right] = 1$ and $m = \frac{\ln|A|}{\ln a_0} = 1$, we see that the match is perfect with only one coefficient. This is possible because the time-scale representation is structured exactly as y in (19), and therefore this representation will be the sparsest possible. In setting the parameters a_0 and b_0 as we did, however, we assumed that we have full information about the motion of both the transmitter and the receiver; in

time	$\hat{h}_n(t) = \frac{1 - v_x/c_0}{d_0 - (v_x - v_y)t} \mathrm{sinc}\left[W \frac{d_0 - (v_x - v_y)t}{c_0 - v_x} - n \right]$
time-frequency	$\hat{S}_{m,n} = \int_{\frac{d_0 - T(v_x - v_y)}{c_0 - v_x}}^{\frac{d_0}{c_0 - v_x}} \frac{\lvert C \rvert}{c_0 \tau T} e^{j 2\pi m \frac{(c_0 - v_x)\tau - d_0}{T(v_x - v_y)}} \mathrm{sinc}[n - \tau W] \mathrm{d}\tau$
time-scale	$\hat{\mathcal{L}}_{m,n}(t) = \sqrt{\lvert A \rvert} \frac{1 - v_x/c_0}{d_0 - (v_x - v_y)t} \mathrm{sinc}\left[\frac{\ln \lvert A \rvert}{\ln a_0} - m \right] \mathrm{sinc}\left[\frac{d_0}{b_0(c_0 - v_x)} - n \right]$

Table 2: Summary of discrete coefficients for the classic Doppler effect.

practice, this may be difficult to obtain. In a previous paper [10], we investigated (albeit very briefly) the consequences of the misestimation of the velocities in the reconstruction.

Finally, Figure 3 shows the time-frequency reconstruction; this representation has the big advantage that, in contrast to the previous 2, its discrete coefficients do not depend on time; so we can represent a time-varying channel in a time-invariant way. However, even for such a simple channel we are unable to obtain the coefficients explicitly, as shown in Table 2, and we need to evaluate them numerically. This can be done quite easily, and we see that, for the given parameters, reconstructing by 1 coefficient only works quite well, whereas using 3 we get almost perfect reconstruction. The largest coefficient here corresponds *approximately*, once more according to Table 2, to $n = W \frac{d_0}{c_0 - v_x}$; also, for simplicity, we used $\omega_0 = 0$ here, so that $\hat{S}_{mn} = 0$ if $m \neq 0$.

What we observe here remains true for a wide range of the parameters as well: in particular, the reconstructions seem to behave as we described above, and give perfect matches for a wide range of the pulse parameters ω_0 and s that we tested, provided we use a sufficient number of coefficients (for example, as T increases in the time-frequency representation, while W is kept fixed, more coefficients are needed). The underlying assumptions about the appropriate content of the signals for which the channel is representable by countable discrete coefficients in its various representations suggest, of course, that one or more of the representations may fail to reconstruct perfectly, no matter how many coefficients we use, if the time, frequency, or scale content of the signal is excessive. Whether this phenomenon can be observed using Gabor signals is an interesting question, but we defer its answer to future work.

6. SUMMARY

In conclusion, we make the following preliminary observations for the reconstruction of Gabor signals:

- The time-domain channel model reconstruction seems to be reasonably sparse, and its coefficients depend on time.
- The time-scale channel model reconstruction also involves time-varying coefficients, and depends on a bijective matching of signal parameters to channel parameters. Perfect efficiency is possible (100% with one coefficent) if the channel parameters are known.
- The time-frequency channel model coefficients are time-invariant, but their determination is a bit more involved; the reconstruction is as sparse as the time domain one for Gabor signals, however, if not sparser.

In continuing work, we will analyze more thoroughly the dependence of the efficiency on signal parameters (such as bandwidth, as all three models assume bandlimited transmit signals) and channel parameters. Additionally, we will look into the issue of signaling efficiency (the loss in signal efficiency associated with the signal parameter assumptions), which was not considered in this work.

References

[1] A. Sayeed and B. Aazhang, "Joint multipath-Doppler diversity in mobile wireless communications," *IEEE Transactions on Communications*, vol. 47, no. 1, pp. 123–132, January 1999.

[2] A. R. Margetts and P. Schniter, "Joint scale-lag diversity in mobile ultra-wideband systems," in *Proceedings of the Thirty-Eighth Asilomar Conference on Signals, Systems and Computers*, Nov. 2004.

[3] Y. Jiang and A. Papandreou-Suppappola, "Time-scale canonical model for wideband system characterization," in *Proceedings of the IEEE International Conference on Acoustics, Speech, and Signal Processing*, Mar. 2005.

[4] S. Rickard, R. Balan, V. Poor, and S. Verdu, "Canonical time-frequency, time-scale, and frequency-scale representations of time-varying channels," *Journal on Communications in Information and Systems, Special Issue Dedicated to the 70th Birthday of Thomas Kailath: Part II*, vol. 5, no. 2, pp. 197–226, Nov. 2005.

[5] T. Kailath, "Sampling models for linear time-variant filters," Massachusetts Institute of Technology, Tech. Rep. "Research Laboratory of Electronics, Technical Report No. 352", May 1959, M.S. thesis, M.I.T. Dept. of Electrical Engineering.

[6] L. A. Zadeh, "Time-varying networks, I," *Proceedings of the IRE*, vol. 49, pp. 1488–1502, October 1961.

[7] T. Kailath, "Measurements on time-variant communications channels," *IRE Transactions on Information Theory*, vol. 8, no. 5, pp. "S229–S236", September 1962.

[8] P. A. Bello, "Characterization of randomly time-variant linear channels," *IEEE Transactions on Communication Systems*, vol. CS-11, no. 4, pp. 360–393, Dec. 1963.

[9] H. L. V. Trees, *Detection, Estimation, and Modulation Theory, Part III.* New York: John Wiley & Sons, 1971.

[10] S. Rickard, K. Drakakis, and N. Tsakalozos, "On the efficiency of time-varying channel models," in *40th Annual Conference on Information Sciences and Systems (CISS)*, Princeton, NJ, March 22–24 2006.

[11] D. Kleppner and R. Kolenkow, *An Introduction to Mechanics.* New York: Mc-Graw-Hill, 1973.

[12] S. Rickard, "Time-frequency and time-scale representations of doubly spread channels," Ph.D. dissertation, Princeton University, Nov. 2003.

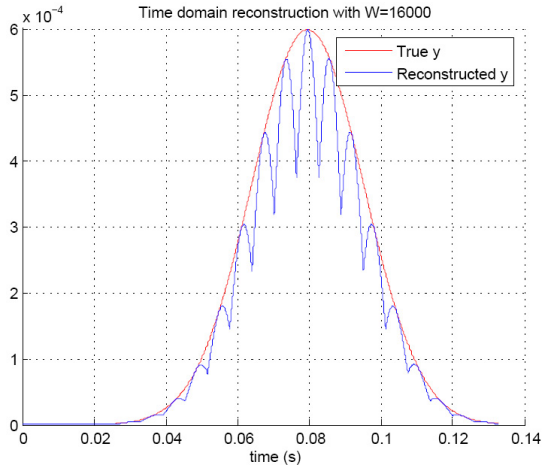

(a)

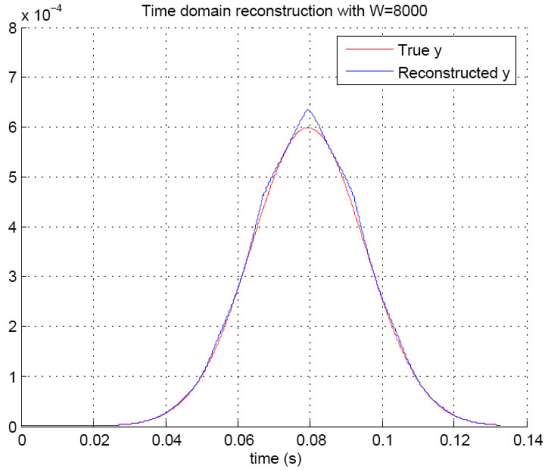

(b)

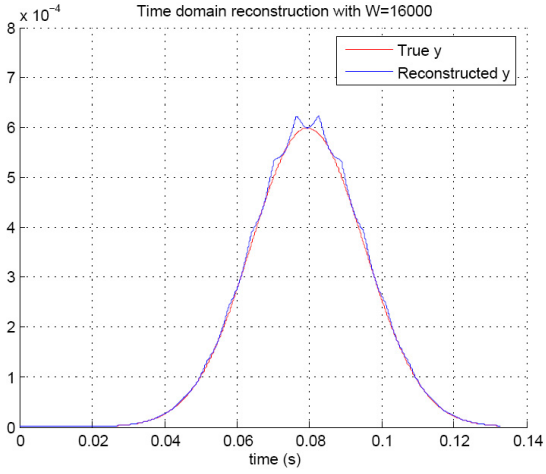

(c)

Figure 1: Time domain reconstruction: (a) uses 1 coeff. and $W = 16KHz$, (b) uses 3 coeff. and $W = 8KHz$, and (c) uses 3 coeff. and $W = 16KHz$.

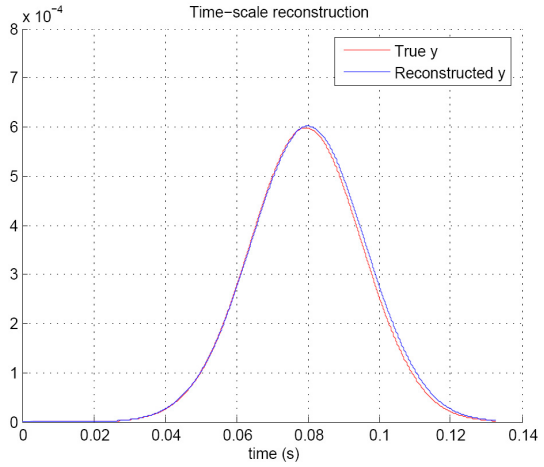

Figure 2: Time-scale reconstruction: we use 1 coeff.

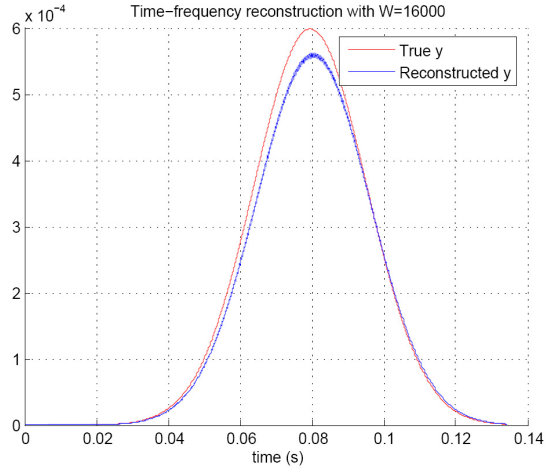

(a)

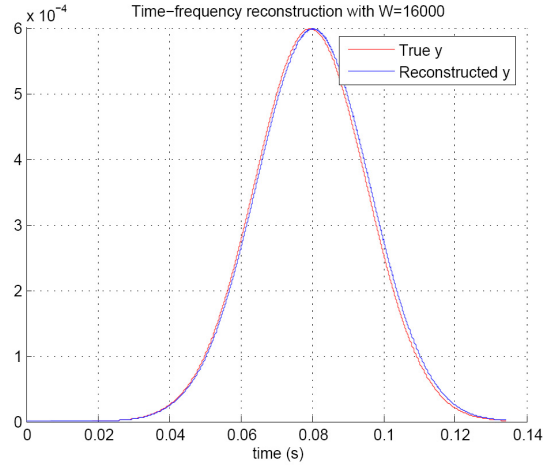

(b)

Figure 3: Time-frequency reconstruction: (a) uses 1 coeff. and $W = 16KHz$, and (b) uses 3 coeff. and $W = 16KHz$. In both cases $T = \frac{2}{W}$.